The prompt x-ray emission of gamma-ray burst 980519

in 't Zand, J.J.M.; Heise, J.; van Paradijs, J.A.; Fenimore, E.

THE PROMPT X-RAY EMISSION OF GAMMA-RAY BURST 980519

J. J. M. IN 'T ZAND,[1] J. HEISE,[1] J. VAN PARADIJS,[2] AND E. E. FENIMORE[3]

ABSTRACT

The prompt X-ray emission from gamma-ray burst (GRB) 980519, as measured with the Wide Field Cameras on board *BeppoSAX*, is characterized by a strong soft-to-hard-to-soft evolution. An analysis of the evolution of the X-ray spectrum in terms of a single power-law model shows that the photon index evolved from −2.0 to −1.1 to −2.4. The onset of the burst has such a soft spectrum that the 2–27 keV emission appears to precede the ≳107 keV emission of GRB 980519 (as measured with the Burst and Transient Source Experiment) by about 70 s. Nevertheless, we show that this early spectral variation is part of a smooth evolution over the whole burst and that there is no convincing evidence that the early X-rays originate from a physical process that is different from that giving rise to the remainder of the burst.

Subject headings: gamma-rays: bursts — X-rays: general

1. INTRODUCTION

The Wide Field Camera (WFC) instrument on board the *BeppoSAX* satellite boosted gamma-ray burst (GRB) research through its capability to localize quickly (within a few hours) and accurately (within a few arcminutes) half a dozen GRBs per year. This enabled for the first time quick and sensitive multiwavelength follow-up observations of a number of GRBs that resulted in the discoveries of X-ray, optical, and radio afterglows (Costa et al. 1997; van Paradijs et al. 1997; Frail et al. 1997). Five optical counterparts have revealed redshifts that, if interpreted as due being to the expansion of the universe, place them at cosmological distances (Metzger et al. 1997; Kulkarni et al. 1998, 1999; Djorgovski et al. 1998b, 1999). A sixth optical counterpart appears to be in a galaxy relatively close to our own (Galama et al. 1998).

Another WFC capability is the measurement of the 2–20 keV X-ray spectrum of GRBs. It is more difficult to exploit this capability than to localize GRBs. In general, the signal-to-noise ratio of the GRB detections with WFC is not high (see, e.g., Heise et al. 1998). A detection may be sufficiently high to image the burst in a broad energy range, but it may be too small if the data are distributed over a good number of photon energy channels. Of the 17 bursts detected with the WFC until 1999 February, about seven give us the opportunity to perform a more elaborate spectral analysis than the determination of the spectral slope over the whole burst alone. Here we discuss one of those seven: GRB 980519. Of all WFC-detected bursts, this burst ranks second in the number of detected photons, after GRB 990123 (Heise et al. 1999) and before GRB 970111 (Feroci et al. 1998).

GRB 980519 triggered the Burst and Transient Source Experiment (BATSE) on the *Compton Gamma Ray Observatory* on 1998 May 19.514035 UT (trigger number 6764). Its 50–300 keV peak flux[4] of 4.72 ± 0.14 photons cm^{-2} s^{-1}, integrated over 256 ms, would place it in the brightest 14% of all bursts in the 4B catalog (Meegan et al. 1998). Simultaneously, the X-ray counterpart to the burst was detected in WFC unit number 2 at an off-axis angle of 7° and localized with an error circle radius of 3′ (Muller et al. 1998). Jaunsen et al. (1998) detected a fading optical counterpart in the WFC error box in *V*- and *I*-band observations that started 8.8 hr after the burst (see also Djorgovski et al. 1998a). A fading X-ray afterglow was detected 9.7 hr after the burst with the narrow-field instruments on *BeppoSAX* (Nicastro et al. 1998a). Frail et al. (1998) report the detection of a brightening 8.3 GHz radio counterpart coincident with the optical counterpart from observations on May 19.8, 20.6, and 22.3. Sakolov et al. (1998) report the detection of an $R = 26.05 \pm 0.22$ extended source that may be the host galaxy. This was confirmed by Bloom et al. (1998).

GRB 980519 is of particular interest because there appears to be X-ray activity prior to the gamma-ray event. In the past, there have been sporadic reports of such activity in other GRBs. The best-documented case is GRB 900126, which was detected with the *Ginga* GRB detectors with 1–370 keV coverage. Murakami et al. (1991) found these data to exhibit clear X-ray emission in the 2–10 keV band about 10 s prior to the onset of the gamma-ray event. It could be modeled by blackbody radiation of temperature $kT = 1.58 \pm 0.26$ keV. Other (less documented) cases of bursts with preburst X-ray activity have been found in *P78-1* data (Laros et al. 1984) and WATCH data (Sazonov et al. 1998). In the WATCH database of 95 GRBs, six appear to have preburst activity. In the *Ginga* database of 121 GRBs, there is the one convincing case and two possible cases (Murakami et al. 1992). This suggests that preburst ≲20 keV activity occurs in only a few percent of the GRBs. Preburst activity in any wavelength regime is considered to be important in constraining the nature of the central engine of the GRBs. For instance, in a recent study, Paczyński (1998) proposes that the preburst X-ray activity in GRB 900126 supports the hypernova scenario for the GRB central engine. In this scenario, rotational energy is extracted from a freshly formed black hole through a torus around it. The preburst blackbody radiation could be due to thermal radiation from this torus.

In this Letter, we study the prompt X-ray emission of GRB 980519. We discuss the question of whether truly preburst X-ray activity is present, and we consider the relationship of the prompt X-ray emission with the X-ray afterglow.

[1] Space Research Organization of the Netherlands, Ruimteonderzoek, Sorbonnelaan 2, Utrecht, CA, NL-3584, the Netherlands; jeanz@sron.nl.

[2] Astronomical Institute "Anton Pannekoek," University of Amsterdam, and Center for High Energy Astrophysics, Kruislaan 403, Amsterdam, SJ, NL-1098, the Netherlands; and Department of Physics, University of Alabama in Huntsville, Huntsville, AL 35899.

[3] Los Alamos National Laboratory, Mail Stop D436, Los Alamos, NM 87545.

[4] As made available in the current BATSE catalog by C. Meegan et al. through http://www.batse.msfc.nasa.gov/data/grb/catalog/.

2. OBSERVATIONS AND ANALYSIS

The WFC instrument (Jager et al. 1997) consists of two coded aperture cameras, each with a field of view of 40° by 40° FWZR and an angular resolution of about 5′. The bandpass is 2–27 keV. The spectral resolution is approximately constant over the bandpass at 20% FWHM. The field of WFC unit 2, in which GRB 980519 was detected, was void of other point-source detections. Therefore, the sensitivity of the observation was dominated by the background, which is an optimum situation. Proper spectral analyses of WFC data are limited to within 2–20 keV because the response function is not yet sufficiently well determined outside that range. Furthermore, a systematic error of ~7% applies per channel. In the case of GRB 980519, the systematic error does not degrade the analysis because the X-ray fluence is so small that statistical errors dominate.

The gamma-ray measurements presented here were obtained from the publicly available archive of BATSE large area detector (LAD; Fishman et al. 1989) data. Specifically, we used the "DISCSC" data product that contains the combined photon count rates of the two LADs (out of eight) that were most favorably oriented toward GRB 980519, in four photon energy channels and with 1.024 s time resolution or better.

2.1. *The* 2 keV *to Greater than* 325 keV *Time Profile*

Figure 1 presents the time profile of the WFC and BATSE data in seven different photon energy bands. These profiles are obtained from photon count rates on detectors, without a correction for the projected area. A number of characteristics catch the eye. First, there is X-ray activity up to several tens of keV preceding the onset of $\gtrsim 107$ keV gamma-ray emission by about 70 s. This pre–gamma-ray activity has a quick rise at about $T = -50$ s (T is the time relative to the BATSE trigger time) and continues into the main peak. It is discernible in all WFC channels, as well as the first BATSE channel, up to 58 keV. Second, there is an X-ray tail present that contains a double-peaked feature that is almost completely separated from the soft emission around the main gamma-ray peak. It continues for another 80 s after the $\gtrsim 107$ keV emission has ended. In the following, we will employ the terms "nose" and "tail" to refer to the 2–27 keV X-ray emission before ($T = -85/-5$ s) and after ($T = 46/120$ s) the main gamma-ray event as measured above ~107 keV.

2.2. *The X-Ray Spectrum*

To study the X-ray spectrum, the data were resolved in 10 time intervals. Spectra were generated by cross-correlating the position information of the detected photons with the aperture mask (see, e.g., Jager et al. 1997). This ensures that the information obtained pertains uniquely to the emission from the GRB position. We stress this because in GRB research it is customary to determine spectra directly from background-subtracted time profiles, such as those shown in Figure 1. Our procedure has a number of advantages with respect to this. It guarantees that source confusion is not an issue, nor scattering effects from within the instrument, spacecraft, or Earth. It makes the generation of the response matrix straightforward, and it keeps the analysis independent from background variation models.

The spectrum can be modeled by a simple power-law function with a low-energy cutoff. In what way exactly the low-energy cutoff is modeled is ambiguous. The following two (commonly used) models are equally successful in describing the data:
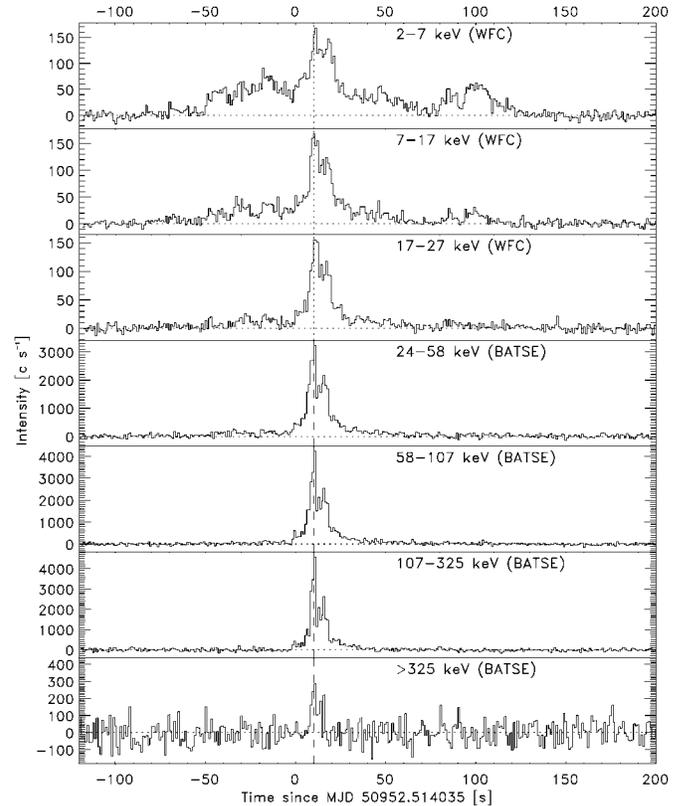

FIG. 1.—Time profile of GRB 980519 in seven bandpasses. The time resolution is 1 s for the WFC data and 1.024 s for the BATSE data. The unit is photon counts per time bin. The background has been subtracted. The time dependency for the background was determined through a linear interpolation between the first and the last 20 s in this plot. The time is relative to the BATSE trigger time. The vertical dashed line is drawn as guidance. The horizontal dotted lines are at intensities of zero. The BATSE bandpass edges are averages of two LAD detectors.

1. A power-law function with absorption due to cold interstellar or circumstellar gas of cosmic abundances:

$$N(E) = K \exp\left[-N_{\rm H}\sigma(E)\right]E^{\Gamma}$$

photons s^{-1} cm^{-2} keV^{-1}, where E is the photon energy, Γ is the photon index, $\sigma(E)$ is the cross section (in units of cm2) per H atom (following Morrison & McCammon 1983), and $N_{\rm H}$ is the hydrogen column density in units of cm^{-2}.

2. The empirical GRB model spectrum as defined by Band et al. (1993):

$$N(E) = \begin{cases} AE^{\alpha}\exp\left(-E/E_0\right), & \text{for } E \leq (\alpha-\beta)E_0, \\ BE^{\beta}, & \text{for } E \geq (\alpha-\beta)E_0 \end{cases}$$

photons s^{-1} cm^{-2} keV^{-1}, where A and B are coupled constants.

We fitted both models. In our pursuit to describe the spectral evolution with as simple a model as possible, we found that the data allow us to fit all 10 temporal samples with a single value for the low-energy parameter (i.e., the low-energy parameters are "tied" over the 10 samples, while the high-energy power-law index is left free). The reduced χ^2, χ^2_r, is 0.91 for

model A (239 degrees of freedom [dof]) and 0.94 for model B (238 dof). The results for the high-energy index are presented in Figure 2 for model A (i.e., Γ). The high-energy index values are similar in the two models. The evolution of Γ is a mirror of the time profile in Figure 1. The soft onset and tail are characterized by $\Gamma = -1.6 \pm 0.2$ at $T = -80$ s to $\Gamma = -2.4 \pm 0.2$ at $T = 80$ s. The main intensity peak is characterized by a peak in Γ as well of -1.0 ± 0.1. If the evolution is simplified and the power-law indices are tied over the three intervals covering $T = -85/-5$ s (comprising the nose of the burst) and the three intervals covering $T = 46/120$ s (tail), the data are still well described, with $\chi_r^2 = 0.92$ for 243 dof for model A. The photon index Γ is -2.01 ± 0.09 for the nose and -2.34 ± 0.11 for the tail. Apparently, the evidence for a spectral softening outside the main gamma-ray event is marginal.

The low-energy cutoff in model A is $N_H = (3.7 \pm 0.5) \times 10^{22}$ cm^{-2}, which is about 20 times larger than the local Galactic value (as interpolated from the maps by Dickey & Lockman 1990). It is also in contrast to the optical counterpart that shows no strong extinction (Gal et al. 1998). The disagreement with the value for the X-ray afterglow [$N_H = (0.3-2) \times 10^{22}$; Nicastro et al. 1998b] is a factor of ~3. These differences could be due to either variable absorption or an inappropriate interpretation of the cutoff as absorption. The true nature of this cutoff is not important to the conclusions of this Letter.

The total 2–10 keV fluence is 1.8×10^{-6} ergs cm^{-2}, and that in 2–20 keV is 3.1×10^{-6} ergs cm^{-2}. The latter is roughly 30% of the fluence between 2 and 300 keV [it is $(6.89 \pm 0.08) \times 10^{-6}$ ergs cm^{-2} for 25–300 keV; see footnote 4].

3. DOES GRB 980519 EXHIBIT PREBURST X-RAY ACTIVITY?

The early X-ray emission in the nose prompts the question of whether it can be attributed to a fundamentally different emission mechanism than is operating during the main gamma-ray event, and thus possibly constrains models for the central engine, or whether it is merely an exhibition of an initial soft-to-hard spectral evolution of one physical process. In other words, does GRB 980519 exhibit preburst X-ray activity? We regard the answer to be positive when the emission in the nose cannot be described by the same spectral model as the emission of the main gamma-ray phase or when the spectral parameter values of the X-ray phase are (near to) unprecedented for GRBs while those of the gamma-ray phase are not.

The spectral analysis of GRB 980519 clearly shows that the spectrum can be described by the same model throughout the burst. Thus, the first criterion for preburst X-ray activity does not hold for GRB 980519. This is in contrast to the best-documented case of preburst X-ray emission so far, GRB 901126 (Murakami et al. 1991). The soft start of that burst could be modeled by blackbody radiation ($\chi_r^2 = 1.6$ for 12 dof) and not by a power-law function ($\chi_r^2 = 3.6$ for 12 dof) nor by thermal bremsstrahlung ($\chi_r^2 = 2.1$ for 12 dof), while the spectrum of the gamma-ray phase could be described well by thermal bremsstrahlung. For GRB 980519, blackbody spectral models are excluded at high levels of confidence by the nose data. The best fit for $T = -50/-5$ s has a $\chi_r^2 = 3.86$ (23 dof). We note that there is yet another difference between GRB 980519 and GRB 900126, which relates to the variability of the initial X-ray emission. In GRB 900126, this emission increases smoothly until the peak, while in GRB 980519, there is more structure in the initial X-ray phase.

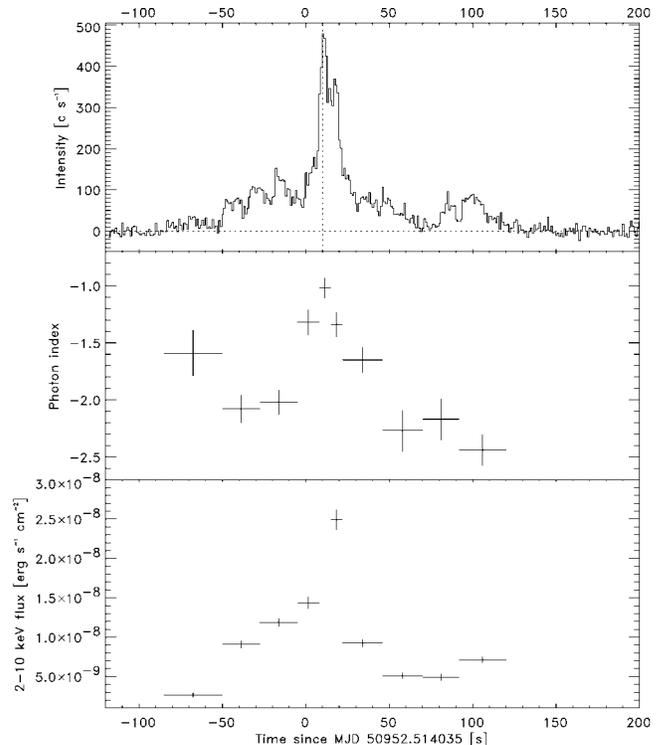How does the spectrum of the nose of the GRB 980519

FIG. 2.—The top panel shows the history of the photon count rate over the full WFC bandpass; the middle panels shows the evolution of the X-ray photon index over the burst; and the bottom panel shows the history of the 2–10 keV flux.

compare with that of other GRBs? Systematic spectral measurements of GRBs that include data below ~10 keV have so far only been performed with the *Ginga*-GBD and the *BeppoSAX*-WFC. The total number of bursts detected is 121 for *Ginga*-GBD and 17 for *BeppoSAX*-WFC. Strohmayer et al. (1998) studied the overall spectra of the 22 brightest *Ginga* bursts in terms of model B. Seven of these bursts have break energies $(\alpha - \beta)E_0$ below 10 keV (it is ~5 keV for GRB 980519). Among these seven bursts, the softest spectrum has $\beta = -2.26 \pm 0.14$ [and $\alpha = 0.22$ and $(\alpha - \beta)E_0 = 9.1$ keV]. This is, within the error margins, equal to what is seen in the nose of GRB 980519. Therefore, the second criterion for preburst X-ray activity also does not hold for GRB 980519.

We conclude that, despite the suggestive time profiles, there is no strong evidence for preburst X-ray activity in GRB 980519. In our opinion, reports on preburst X-ray activity or X-ray precursors in other bursts based on time profiles alone should be interpreted carefully. This has also been concluded from a systematic study of precursors based solely on BATSE data (Koshut et al. 1995).

4. THE RELATIONSHIP TO THE X-RAY AFTERGLOW

The photon index during the tail is, within the error margins, identical to that of the X-ray afterglow of GRB 980519 of $-2.8_{-0.5}^{0.6}$ (Nicastro et al. 1998b). In fact, this applies in a more general sense as well. First, this index is quite common for many tail spectra of GRBs: BATSE data reveal that for 22 GRBs that were followed up in X-rays, the tail spectra have an average low-energy photon index of -1.9 ± 0.4 (Koshut et al. 1999). Second, the index is common to what is observed on average in seven cases of X-ray afterglows (-2.2 ± 0.4;

Owens et al. 1998). The X-ray spectrum of the tail is also quite similar to that of the nose and in contrast to the gamma-ray phase.

The similarity of the spectra in the nose, tail, and X-ray afterglow may lead one to suggest that the nose and tail emission have the same origin as the X-ray afterglow and a different one than that of the main gamma-ray event; in other words, that the X-ray afterglow started *before* the burst. An explanation would have to be searched in terms of the very successful fireball model (for a recent review and list of references, see Piran 1998). This model infers that the afterglow is due to external shocks (which result from the interaction of the fireball with the surrounding medium) and that the burst is due to internal shocks (which result from the interaction between different parts of the fireball). An early start of the X-ray afterglow would involve particularities of the fireball in GRB 980519 that make external shocks set in prior to internal shocks. However, the considerable structure in the time profile of the nose and tail is unlike that expected for external shocks (as has been argued in general for GRB time profiles by Fenimore, Madras, & Nayakshin 1996), and an interpretation in terms of an X-

ray afterglow preceding the gamma-ray burst must currently be considered speculative at best.

5. CONCLUSIONS

We have presented the intriguing characteristics of the prompt X-ray emission from GRB 980519 and briefly speculated on the implications. GRB 980519 is characterized by a strong soft-to-hard-to-soft evolution, each of these three stages lasts between 50 and 80 s. Although suggestive of preburst X-ray activity, the soft start of the burst evolves smoothly into the main gamma-ray event through variations of the parameters of a single spectral model. Thus, there is no reason to assume that the emission mechanism is fundamentally different during the soft start. Furthermore, the similarity of nose, tail, and X-ray afterglow spectra suggests that they have a common origin. However, the type of variability of these soft stages does not support such a far-reaching conclusion.

REFERENCES

Band, D., et al. 1993, ApJ, 413, 281
Bloom, J. S., Kulkarni, S. R., Djorgovski, S. G., Gal, R. R., Eichelberger, A., & Frail, D. A. 1998, GCN Circ. 149
Costa, E., et al. 1997, Nature, 387, 783
Dickey, J. M., & Lockman, F. J. 1990, ARA&A, 28, 215
Djorgovski, S. G., Gal, R. R., Kulkarni, S. R., Bloom, J. S., & Kelly, A. 1998a, GCN Circ. 79
Djorgovski, S. G., Kulkarni, S. R., Bloom, J. S., Frail, D., Chaffee, F., & Goodrich, R. 1999, GCN Circ. 189
Djorgovski, S. G., Kulkarni, S. R., Bloom, J. S., Goodrich, R., Frail, D. A., Piro, L., & Palazzi, E. 1998b, ApJ, 508, L17
Fenimore, E. E., Madras, C. D., & Nayakshin, S. 1996, ApJ, 473, 998
Feroci, M., et al. 1998, A&A, 332, L29
Fishman, G. J., et al. 1989, in Proc. GRO Science Workshop, ed. W. N. Johnson (Greenbelt: NASA/GSFC), 2
Frail, D. A., Kulkarni, S. R., Nicastro, L., Feroci, M., & Taylor, G. B. 1997, Nature, 389, 261
Frail, D. A., Taylor, G. B., Kulkarni, S. R., & *BeppoSAX* GRB Team. 1998, GCN Circ. 89
Gal, R. R., Bloom, J. S., Djorgovski, S. G., & Kulkarni, S. R. 1998, GCN Circ. 92
Galama, T. J., et al. 1998, Nature, 395, 670
Heise, J., et al. 1998, in AIP Conf. Proc. 428, Gamma-Ray Bursts, ed. C. A. Meegan, R. D. Preece, & T. M. Koshut (New York: AIP), 397
———. 1999, in preparation
Jager, R., et al. 1997, A&AS, 125, 557
Jaunsen, A. O., Hjorth, J., Andersen, M. I., Kjernsmo, K., Pedersen, H., & Palazzi, E. 1998, GCN Circ. 78

Koshut, T. M., et al. 1995, ApJ, 452, 145
———. 1999, in preparation
Kulkarni, S. R., et al. 1998, Nature, 393, 35
———. 1999, Nature, in press (astro-ph/9902272)
Laros, J. G., Evans, W. D., Fenimore, E. E., Klebesaedel, R., Shulman, S., & Fritz, G. 1984, ApJ, 286, 681
Meegan, C., et al. 1998, in AIP Conf. Proc. 428, Gamma-Ray Bursts, ed. C. A. Meegan, R. D. Preece, & T. M. Koshut (New York: AIP), 3
Metzger, M. R., et al. 1997, Nature, 387, 879
Morrison, R., & McCammon, D. 1983, ApJ, 270, 119
Muller, J. M., et al. 1998, IAU Circ. 6910
Murakami, T., et al. 1991, Nature, 350, 592
Murakami, T., Ogasaka, Y., Yoshida, A., & Fenimore, E. E. 1992, in AIP Conf. Proc. 265, Gamma-Ray Bursts, ed. W. S. Paciesas & G. J. Fishman (New York: AIP), 28
Nicastro, L., et al. 1998a, IAU Circ. 6912
———. 1998b, A&AS, in press
Owens, A., et al. 1998, A&A, 339, L37
Paczyński, B. 1998, ApJ, 494, L45
Piran, T. 1998, Phys. Rep., in press (astro-ph/9810256)
Sakolov, V., Zharikov, S., Palazzi, E., Nicastro, L., & SAX-GRB Team. 1998, GCN Circ. 148
Sazonov, S. Y., et al. 1998, A&AS, 129, 1
Strohmayer, T. E., Fenimore, E. E., Murakami, T., & Yoshida, A. 1998, ApJ, 500, 873
van Paradijs, J., et al. 1997, Nature, 386, 686